DEVELOPMENT OF THIRD HARMONIC GENERATION AS A SHORT PULSE PROBE OF SHOCK HEATED MATERIAL

W. Grigsby, B. I. Cho, A. C. Bernstein, H. J. Quevedo, J. Colvin, M. C. Downer, and T. Ditmire

Citation: AIP Conference Proceedings **955**, 1097 (2007); doi: 10.1063/1.2832908
View online: http://dx.doi.org/10.1063/1.2832908
View Table of Contents:
http://scitation.aip.org/content/aip/proceeding/aipcp/955?ver=pdfcov
Published by the AIP Publishing

DEVELOPMENT OF THIRD HARMONIC GENERATION AS A SHORT PULSE PROBE OF SHOCK HEATED MATERIAL

W. Grigsby[1], B. I. Cho[1], A. C. Bernstein[1], H. J. Quevedo[1], J. Colvin[2], M. C. Downer[1], and T. Ditmire[1]

[1]*Texas Center for High Intensity Laser Science, The University of Texas,*
1 University Station C 1510, Austin TX 78712
[2]*Chemistry and materials science, Lawrence Livermore National Lab, Livermore, CA 94550*

Abstract. We are studying high-pressure laser produced shock waves in silicon (100). To examine the material dynamics, we are performing pump-probe style experiments utilizing 600 ps and 40 fs laser pulses from a Ti:sapphire laser. Two-dimensional interferometry reveals information about the shock breakout, while third harmonic light generated at the rear surface is used to infer the crystalline state of the material as a function of time. Sustained third harmonic generation (THG) during a ~100 kbar shock breakout indicate that the rear surface remains crystalline for at least 3 ns. However, a decrease in THG during a ~300 kbar shock breakout suggests a different behavior, which could include a change in crystalline structure.

Keywords: Laser driven shock, time resolved, interferometry, harmonic generation
PACS: 42.65.Ky, 62.20.-x, 62.50.+p, 78.20.-e

INTRODUCTION

The investigation of shock induced phase transitions has been an area of interest for decades. The identification of the phase transition in iron established the shock compression field as a separate and important scientific field in the mid-1950s [1] and it continues to be of scientific interest to this day [2]. In typical experiments, a mechanical object or intense laser beam is incident on a material target, inducing a mechanical shock wave. As the shock wave propagates, it heats and compresses the material to conditions found on the Hugoniot. Diagnostics are typically fielded on the rear surface to measure the shocked state.

To help understand the complex behaviors of shock induced phase transitions, such as melt, we are developing an ultra-fast non-linear optical technique that is sensitive to the crystalline symmetry of the target. Through the use of femtosecond laser pulses, the time-scale for these transitions can be monitored with high time resolution. In fact, linear and non-linear optical probes have measured the time scale for front-surface femtosecond laser melting of silicon at less than 200 fs [3]. In this case, the solid melts non-thermally, faster than is possible through thermal processes involving electron-phonon coupling (of order picoseconds).

In order to observe the shock driven melt transition, a change from the crystalline material to the disordered (melted) material needs to be observable. To do so, our technique utilizes third harmonic generation (THG) at the rear surface from a circularly polarized femtosecond probe so that the signal is sensitive to the anisotropy of the crystalline material [4,5]. This technique provides structural information within a skin depth of the target surface, and will help provide a more complete understanding of the high-pressure shocked material behavior when included with existing diagnostics such as time-resolved reflectivity, and X-ray diffraction.

EXPERIMENTAL PROCEDURE

These experiments were performed on the THOR laser at the University of Texas at Austin. THOR is a Ti:sapphire CPA laser capable of producing >1 J of energy in a stretched pulse of ~600 ps FWHM. Most of this energy (~700 mJ) is split from the system before compression for use in driving the shock wave at the front surface of the target. The rest of the energy is sent into the compressor, where it is temporally compressed down to 40 fs FWHM and attenuated for use in optically probing the shock expansion at the rear surface. Experiments were of the pump-probe variety, where the relative delay is adjusted between each shot to map out the behavior as a function of time.

The experiments were performed inside of a vacuum chamber to prevent ionization of the atmosphere from the high-intensity laser foci at the target surfaces. The shock-driving laser was focused by adjusting an f/20 lens to achieve spot sizes of order a few tens of microns FWHM. The sizes were varied to achieve peak intensities of 1×10^{13} to 2×10^{14} W/cm^2. This laser pulse drove an

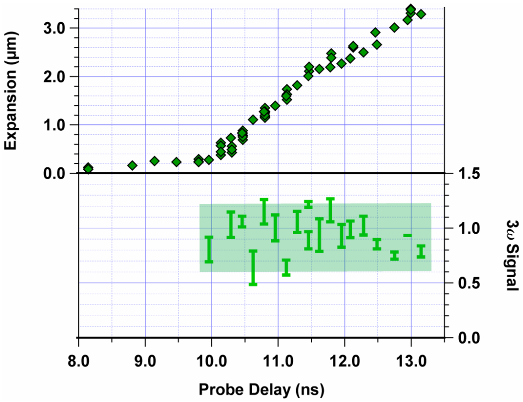

Figure 1 Top: rear surface expansion of 95 µm silicon as a function of probe delay. Bottom: normalized THG vs. probe delay. The THG signal remains fairly constant throughout the probed expansion of 3 µm. The vertical bars between points are uncertainty bars, which are discussed in the text. The broad horizontal line is only to guide the eye.

ablation-driven shock wave which traveled through the target and expanded out of the rear surface. Our targets consisted of commercial silicon-on-insulator (SOI) wafers that were processed using lithography and an etching process to produce an array of regions thinned down to the base layer. The base layers consisted of silicon, with a thickness of 10 – 95 µm, depending on the wafer. An XYZ translation stage moved the target between shots.

The main diagnostic used to determine particle and shock velocities was a Mach-Zehnder interferometer with one leg reflecting off of the silicon rear surface [6]. The other diagnostic consisted of a circularly polarized pulse at normal incidence on the target back surface. This acted as a nonlinear optical probe to generate THG while the target remained crystalline. The probe is focused to ~20 µm and attenuated to a fluence of order 10 mJ/cm^2 so as to stay below the damage threshold for Si. THG is expected for cubic materials, but not for isotropic materials, or upon melting, which alters the index of refraction for liquid silicon. The signal is filtered with several interference filters and measured using a PMT.

RESULTS AND DISCUSSION

The analysis of interferometric data was performed with Fourier analysis of the fringes, as discussed elsewhere [6]. The third harmonic intensity was normalized relative to reference shots taken on clean regions of the target seconds before the actual shot.

The data presented in **Figure 1** were taken using 95 µm silicon shocked with laser intensities of 2×10^{13} and 6×10^{13} W/cm^2. These experiments, in contrast with the data discussed below, created a large shock breakout (~100 µm wide at 1 µm expansion). This is due to the two-dimensional spreading of the decaying shock wave as it propagated through the target. This larger size allowed much cleaner interferometric images to be obtained, and led to less scatter in the data.

The lack of surface expansion dependence on incident laser intensity indicates that the shock velocity and particle velocity for this breakout are independent of pressure over the range tested. This occurs if the shock breakout is from an elastic wave. This conclusion agrees with the measured

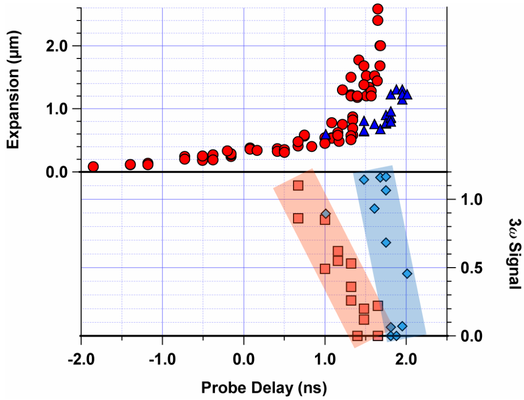

Figure 2. Top: plot of rear surface expansion of 20 µm (circles) and 30 µm (triangles) silicon as a function of probe delay. Bottom: plot of normalized THG vs. probe delay. The THG signal decreases for both target thicknesses. The broad lines are only to guide the eye.

free surface velocity of ~1.1 km/s, which corresponds to a pressure of ~100 kbar, found by comparison with published Hugoniot data [7].

The third harmonic data from 95 µm Si were compromised by the inclusion of scattered target self-emission or plasma light. This fact leads to an uncertainty in the actual THG signal, the range of which is indicated as uncertainty bars in **Figure 1**. The range for each shot depends on the amount of background level, with the upper end assuming a background of zero, and the lower end assuming a background equal to the maximum level for that shot.

This data show that the THG signal remains fairly constant throughout most of the target expansion. From this, we conclude that the material is remaining crystalline during the shock breakout for at least the first 3 µm of expansion. The crystalline structure is expected for an elastic shock break-out, but the data actually confirms this hypothesis.

The data shown by circles in **Figure** 2 represent data taken with 20 µm targets and an incident pump intensity of I = 2x10^{13} W/cm^2. These data show the transition from motion due to target pre-expansion to motion due to shock breakout occurring near the 0.6 µm expansion point. The pre-expansion has a free surface velocity of ~0.14 km/s while the shocked free surface velocity is ~4 km/s. Using the free surface approximations leads to a particle velocity of ~2 km/s, corresponding to a shock pressure of ~300 kbar.

The triangles in **Figure** 2 represent data from 30 µm targets and an incident pump intensity of I = 1x10^{14} W/cm^2. These data cover the temporal regions of the end of the pre-expansion and the very beginning of the shock expansion. The data in this run is too scattered to estimate a reliable free-surface velocity and pressure. However, comparison of these data with other data (not plotted) leads to a range for the shock velocity of 6-10 km/s, which surround the elastic sound speed of ~9 km/s for (100) silicon. More statistics are needed to improve the accuracy of this velocity estimate.

In contrast to data taken with 95-µm thick targets, the 20-µm and 30-µm thick targets both resulted in a decrease in THG signal. The 20-µm target data even seem to indicate that the THG begins to decrease just before the shock wave reaches the rear surface. To explain this unexpected result, we consider the possibility that some of this drop in THG signal could be due to a variety of possible causes.

One possible cause for a drop in our THG signal would be if the expanding target topography deflects our probe beam outside the collection cone of our f/3 optics. For example, with the spatial size of the shock expansion is approximately the same as the probe laser spot size (~20 µm) it is possible that shot-to-shot pointing variation causes the laser spot to hit the side of the shock expansion so that the third harmonic is generated from the sloped region of the expansion, rather than from the peak. This could potentially send the third harmonic light, which is emitted in the specular reflection direction, outside of the collection optics. Using the interferometric data for our shots, however, we determine that peak target slope, plotted in the bottom of **Figure** 3, was too small to explain the entire drop in the 30-µm target data, and none of the drop in the 20-µm target data. Therefore, other mechanisms must be causing the majority of decreased THG signal.

Another complication of the non-planar target expansion is that the angle of incidence of the probe pulse that generates the third harmonic changes as the target slope changes. This change in angle affects the harmonic generation through the linear and nonlinear Fresnel equations [4].

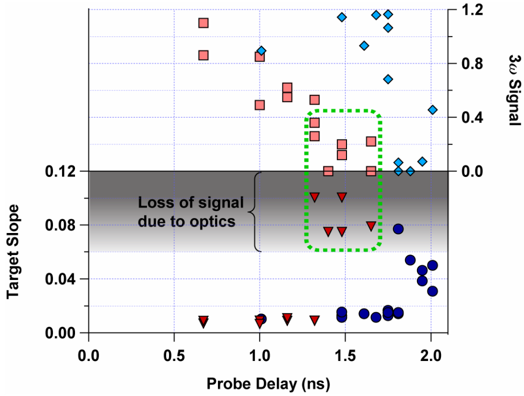

Figure 3. Top: plot of the THG signal for 20 µm (squares) and 30 µm (diamonds) Si as a function of probe delay. Bottom: plot of the peak target slope as calculated from the interferometric data as a function of probe delay. The gray shaded region indicates the range of target slopes that reflect some light outside of the collection optics. The dark gray region above 0.1 slope indicates the expected region of complete loss of collected light. The dashed bounding box encompasses data that can possibly be explained by the loss of light from the collection optics.

However, calculations show that the third harmonic intensity changes less than 2% for angles less than 5°, or target slopes less than 0.09.

Another possibility is that the index of refraction could be changing between 100 and 300 kbar, which would alter the THG through the Fresnel equations. However, previous research shows that the conductivity of Si changes minimally between these two pressures, indicating that a change in index of refraction is not expected [8].

Because the rear surface of the target is expanding at high velocity into vacuum, we cannot yet rule out the possibility that particles and/or a plasma develop upon shock breakout. Future experiments are planned to obtain reflectivity data at normal incidence for comparison with this THG data so that we may determine if the probe light is being scattered, or if the THG drop is due to another effect, such as a change in the crystalline symmetry affecting the nonlinear susceptibility. However, a loss of crystalline order is not expected until Mbar pressures are attainted, where silicon is expected to melt on the Hugoniot.

CONCLUSIONS

Laser produced shock waves in (100) Si wafers were studied using femtosecond laser pulses. Two-dimensional displacement interferometry was used to characterize the rear surface expansion as a function of time, while third harmonic generation using a circularly polarized probe revealed information on the symmetry of the crystalline lattice. A distinct change in THG is noticed between targets shocked to ~100 kbar, and those shocked to ~300 kbar. The THG remains constant during the 100 kbar shock breakout, indicating that the silicon is remaining crystalline. However, THG from the 300 kbar shock breakout decreases on the nanosecond timescale, possibly due to a change in the crystalline structure. Future experiments will focus on determining the precise cause of the THG drop.

This work was supported by the Army Research Office and the National Nuclear Security Administration under cooperative agreement DE-FC52-03NA00156.

REFERENCES

1. Bancroft, D., Peterson, E. L., and Minshall, S., Journal Of Applied Physics **27** (3), 291 (1956); Walsh, J. M., Bulletin of the American Physical Society **29**, 28 (1954).
2. Kadau, K., Germann, T. C., Lomdahl, P. S. et al., Physical Review Letters **98** (13) (2007); Kalantar, D. H., Collins, G. W., Colvin, J. D. et al., International Journal of Impact Engineering **33** (1-12), 343 (2006).
3. Tom, H. W. K., Aumiller, G. D., and Brito-Cruz, C. H., Physical Review Letters **60** (14), 1438 (1988).
4. Burns, W. K. and Bloembergen, N., Physical Review B (Solid State) **4** (10), 3437 (1971).
5. Yakovlev, V. V. and Govorkov, S. V., Applied Physics Letters **79** (25), 4136 (2001).
6. Grigsby, W., Bowes, B. T., Dalton, D. A. et al., in *Shock Compression of Condensed Matter*, edited by M. D. Furnish, M. Elert, T.P. Russell et al. (American Institute of Physics, Baltimore, MD, 2005), Vol. 845, pp. 1337.
7. Goto, T., Sato, T., and Syono, Y., Japanese Journal of Applied Physics Part 2-Letters **21** (6), L369 (1982).
8. Gilev, S. D. and Trubachev, A. M., Journal of Physics: Condensed Matter **16** (46), 8139 (2004).